The Geological Society of America
Special Paper 425
2007

Remotely triggered earthquakes following moderate main shocks

Susan E. Hough
U.S. Geological Survey, 525 S. Wilson Avenue, Pasadena, California 91106, USA

ABSTRACT

Since 1992, remotely triggered earthquakes have been identified following large (M > 7) earthquakes in California as well as in other regions. These events, which occur at much greater distances than classic aftershocks, occur predominantly in active geothermal or volcanic regions, leading to theories that the earthquakes are triggered when passing seismic waves cause disruptions in magmatic or other fluid systems. In this paper, I focus on observations of remotely triggered earthquakes following moderate main shocks in diverse tectonic settings. I summarize evidence that remotely triggered earthquakes occur commonly in mid-continent and collisional zones. This evidence is derived from analysis of both historic earthquake sequences and from instrumentally recorded M5–6 earthquakes in eastern Canada. The latter analysis suggests that, while remotely triggered earthquakes do not occur pervasively following moderate earthquakes in eastern North America, a low level of triggering often does occur at distances beyond conventional aftershock zones. The inferred triggered events occur at the distances at which SmS waves are known to significantly increase ground motions. A similar result was found for 28 recent M5.3–7.1 earthquakes in California. In California, seismicity is found to increase on average to a distance of at least 200 km following moderate main shocks. This supports the conclusion that, even at distances of ~100 km, dynamic stress changes control the occurrence of triggered events. There are two explanations that can account for the occurrence of remotely triggered earthquakes in intraplate settings: (1) they occur at local zones of weakness, or (2) they occur in zones of local stress concentration.

Keywords: earthquake, triggering, aftershock dynamic stress.

INTRODUCTION

In 1992, the Landers earthquake provided unambiguous evidence that the "reach" of a large earthquake can extend far beyond its immediate aftershock zone (e.g., Hill et al., 1993; Bodin and Gomberg, 1994). A similar burst of regional seismicity followed the 16 October, 1999, Mw 7.1 Hector Mine, California earthquake (Gomberg et al., 2001; Glowacka et al., 2002; Hough and Kanamori, 2002). In these and other documented cases, triggered seismicity was observed to occur preferentially, although not exclusively, in active geothermal and volcanic regions, such as Long Valley Caldera, The Geysers, and the Salton Sea region (e.g., Stark and Davis, 1996; Gomberg and Davis, 1996; Prejean et al., 2005). Triggering has also been observed at geothermal and volcanic sites elsewhere around the world (e.g., Power et al., 2001), leading some to conclude that triggered earthquakes are not observed in other seismotectonic settings (Scholz, 2003).

A number of previous studies have presented compelling evidence that remotely triggered earthquakes are caused by the dynamic stress changes associated with transient seismic waves, typically the high-amplitude S and/or surface-wave arrivals (e.g., Gomberg and Davis, 1996; Kilb et al., 2000). The asso-

Hough, S.E., 2007, Remotely triggered earthquakes following moderate main shocks, *in* Stein, S., and Mazzotti, S., ed., Continental Intraplate Earthquakes: Science, Hazard, and Policy Issues: Geological Society of America Special Paper 425, p. 73–86, doi: 10.1130/2007.2425(06).

ciation of triggered earthquakes with dynamic stress changes is in contrast to aftershocks, which appear to be caused primarily by local, static stress changes associated with fault movement (e.g., Das and Scholz, 1981; King et al., 1994; Toda and Stein, 2003). (According to convention, aftershocks are generally, albeit vaguely, assumed to be events within 1–2 fault lengths of a main shock.) Recent studies (e.g., Felzer and Brodsky, 2006) suggest that dynamic stress changes might also play an important role in controlling the distribution of aftershocks. While both types of stress change may play a role in aftershock generation, investigations of remotely triggered earthquakes have focused only on dynamic stress changes.

Because almost all of the initial examples of remotely triggered earthquakes were in regions with active volcanic processes or shallow hydrothermal activity—both of which are associated with abundant heat and fluids at shallow depths in Earth's crust—initially proposed triggering mechanisms involved disruption of fluids. Proposed triggering mechanisms involved the effects of seismic waves on bubbles within fluid systems, such as advective overpressure (Linde et al., 1994) and rectified diffusion (Sturtevant et al., 1996; Brodsky et al., 1998). More recently, Brodsky and Prejean (2005) proposed a barrier-clearing model whereby long-period waves generate fluid flow and pore-pressure changes within fault zones.

In this paper, I summarize both previous and new results that provide compelling evidence that remotely triggered earthquakes do occur following even moderate (M5–7) main shocks outside of active geothermal and/or hydrothermal regions, including intraplate regions.

TRIGGERED EARTHQUAKES IN DIVERSE TECTONIC SETTINGS

To facilitate the subsequent discussion of the implications of remotely triggered earthquake results, in this section, I present both new analyses as well as a brief discussion of salient results from previous studies of remotely triggered earthquakes outside of active geothermal or volcanic regions. In addition to the cases listed next, Gomberg et al. (2004) recently concluded that remotely triggered earthquakes occurred in western North America following the 2002 M7.9 Denali earthquake, although at least some of these events appear to have occurred in or near active geothermal regions.

Central and Eastern North America

Investigations of remotely triggered earthquakes in mid-plate settings are inevitably hampered by data limitations. Researchers are typically limited to analysis of macroseismic data from large historic earthquakes or sparse instrumental data from moderate recent earthquakes. Hough (2001) and Hough et al. (2003) presented evidence for remotely triggered earthquakes that occurred both during the 1811–1812 New Madrid earthquake sequence and following the 1886 Charleston, South Carolina, earthquake. These results suggest that triggering commonly occurs following large earthquakes in the North American mid-continent. There is particularly compelling evidence that moderate earthquakes were triggered in northern Kentucky–southern Ohio during the New Madrid sequence, along or near the Ohio River Valley (Fig. 1). Additionally, Mueller et al. (2004) presented evidence that one of the so-called New Madrid main shocks, conventionally placed in the northern New Madrid seismic zone (e.g., Johnston, 1996; Johnston and Schweig, 1996), may have in fact occurred in the Wabash Valley, ~200 km away from the New Madrid seismic zone.

In retrospect the results of Seeber and Armbruster (1987) also provide evidence that intraplate triggering is common. Although this study talks about "aftershocks" of the 1886 Charleston, South Carolina, earthquake, their inferred locations are distributed over distances of 200–300 km, well outside an expected aftershock zone given the size of the main shock. The triggered events following the Charleston main shock discussed by Hough et al. (2003) were located at even greater distances, for example in the Wabash Valley.

To explore the possibility that remotely triggered earthquakes occur following moderate intraplate earthquakes, I consider recent M4.9–6.1 events in eastern Canada. The Geological Survey of Canada (GSC) operates a network of over 100 seismometers throughout Canada, with especially dense coverage in seismically active areas such as the Charlevoix, Quebec, region of the St. Lawrence Valley. The Canadian National Earthquake Database includes historic earthquakes as far back as 1568, but to focus on earthquakes for which good instrumental data is available, I searched the catalog for M4.9 and greater earthquakes since 1985. The catalog includes 15 such events, the largest two of which are the 1988 Saguenay, Quebec, and the 1989 Ungava earthquakes, both close to M6. Three of the events were in the northernmost United States: since they were recorded in Canada, presumably the network coverage of such events was not ideal. Several earthquakes also occurred in northeastern Canada, where network coverage is presumably also limited. Of the 15 events, 8 occurred in regions where the network should have provided good coverage of small earthquakes (Table 1)

The issue of catalog completeness arises in any seismicity study. In this study, completeness is expected to vary not only with time, but also spatially. However, detecting short-term seismicity fluctuations requires only short-term catalog stability, which can be assumed. One completeness-related issue bears mention, however: completeness invariably degrades in the immediate aftermath of a large regional earthquake. This will hinder the detection of very early triggered earthquakes, in any time or region.

Using catalogs from one month (30 d) before and after each event, I investigated seismicity changes using a standard beta-statistic approach (Matthews and Reasenberg, 1988; Reasenberg and Simpson, 1992). The beta statistic, β, is defined as

$$\beta = N_a - N_e/(v)^{1/2}, \quad (1)$$

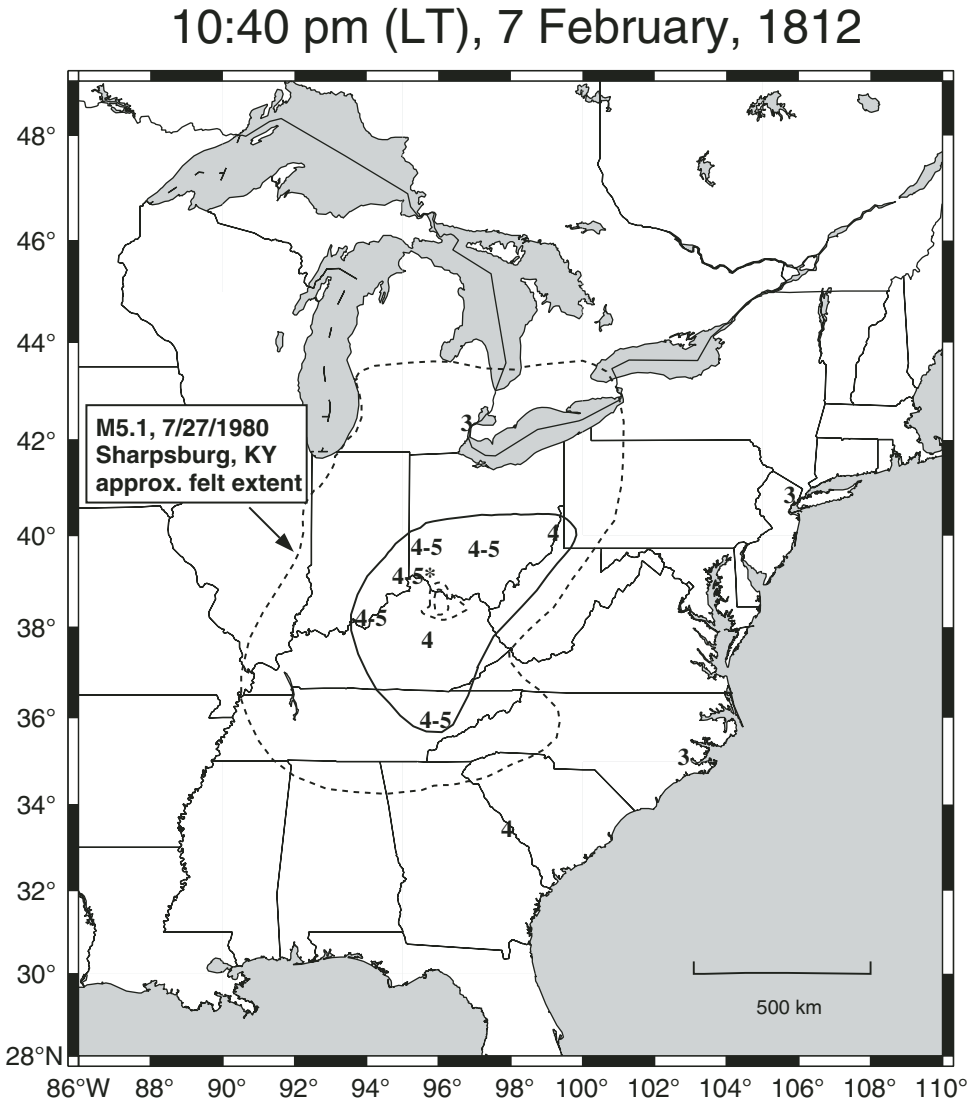

Figure 1. Map showing intensity (MMI) values for an earthquake that occurred at 10:40 p.m. (LT) on 7 February 1812. Within the solid contour, almost all of the accounts describe the event with the word "violent" or "severe." For comparison, the inner dashed lines indicate the MMI V and VI contours for the 1980 M5.1 Sharpsburg, Kentucky, earthquake (Mauk et al., 1982). The outer dashed line indicates the felt area of the Sharpsburg event, which is considerably smaller than that of the 1812 event.

TABLE 1. RECENT MODERATE EARTHQUAKES IN EASTERN CANADA, PLUS THE 2002 AU SABLE FORKS EARTHQUAKE IN NORTHERN NEW YORK STATE

Event	Date	Name	ML	Lat. (°N)	Long. (°W)
1	25 November 1988	Saguenay	6.1	48.12	71.18
2	16 March 1989	Ungava	5.7	60.06	70.06
3	25 December 1989	Ungava(2)	6.1	60.12	73.60
4	18 October 1990	Quebec	5.0	46.47	75.59
5	16 November 1997	St. Lawrence	5.1	46.80	71.42
6	16 March 1999	Quebec(2)	5.1	49.61	66.32
7	1 January 2000	Quebec(3)	5.2	46.84	78.93
8	20 April 2002	Au Sable, NY	5.5	44.53	73.73

Note: Locations and magnitudes (ML) were taken from the Geological Survey of Canada database (http://www.seismo.nrcan.gc.ca/EarthquakesCanada.html).

where N_a is the number of events occurring following an event, N_e is the expected number given the pre–main shock seismicity rates (assuming seismicity is stationary), and v is the variance of N_e. β will be large and positive in regions where seismicity increases. β is correspondingly large and negative in regions where seismicity rate decreases. However, in the "null case," where there are no earthquakes in a given subregion either before or after a main shock, β is not zero. As introduced by Matthews and Reasenberg (1988), N_e represents a probability density function with equal probability over a ±0.5 range bracketing whole numbers. For example, a value of 2 corresponds to an expected range of 1.5–2.5. Because the expected number of earthquakes cannot be negative, if there are zero events in a pre-event window, N_e is set to 0.25. For the analyses in this paper, the baseline value of β is thus not 0 but rather approximately –0.7. β is equal to 0 only if $N_e = N_a$.

Because seismicity levels commonly fluctuate significantly, even a high value of β does not prove that a seismicity increase was caused by a preceding main shock. Other evidence, such as a close temporal correspondence between the main shock timing and the initiation of subsequent events, is needed to establish a causal relationship. This analysis yields no evidence of widespread triggering following any of the events: overall seismicity fluctuations, both positive and negative, appear to be comparable to the usual level of fluctuations observed over time, as illustrated in Figure 2 for a M5.1 event in 1999.

Although the preliminary results are largely negative, several of the beta-statistic maps do reveal a similar feature: an apparent seismicity increase at ~100 km epicentral distance, beyond the presumed aftershock zone for M5–6 earthquakes. To further investigate this result, I calculated the average beta value as a function of epicentral distance from each event. Of the eight earthquakes for which results are shown in Figure 3, five revealed a small increase in β at a distance of ~100 km. None of these small increases was significant by itself, as evidenced by the fact that they are comparable in amplitude to fluctuations seen over the broader region over the same time period. (Also, as noted, even a statistically significant increase would not in itself imply a causal link with the main shock.) What is intriguing, however, is the persistent appearance of a slight increase at a narrow distance range.

The most prominent increase appeared following the mb5.9 1988 Saguenay earthquake. This earthquake was followed within the first month after the main shock by a number of small events along the Charlevoix seismic zone (Fig. 4). The Charlevoix events occurred at relatively shallow depths, whereas the Saguenay source was significantly deeper (Fig. 5). The Charlevoix events were thus clustered in both their epicentral distance from the main shock and their depth distribution. The most straightforward explanation for this clustering is that the events were triggered by postcritical Moho reflections (SmS arrivals), which are known to significantly increase ground motions at a distance of ~100 km. SmS is a body wave, and so SmS-associated triggering would be expected to occur anywhere along the raypath where the wave is of substantial amplitude. If, for example, the Charlevoix events were clustered horizontally but not vertically, this might argue against triggering by body waves. I explore this hypothesis further in a later section.

Northern India

As a second example of triggering outside of geothermal or hydrothermal areas, I summarize recent results from the 1905 Kangra, India, earthquake, for which very early instrumental data are available. The Kangra earthquake has been the subject of

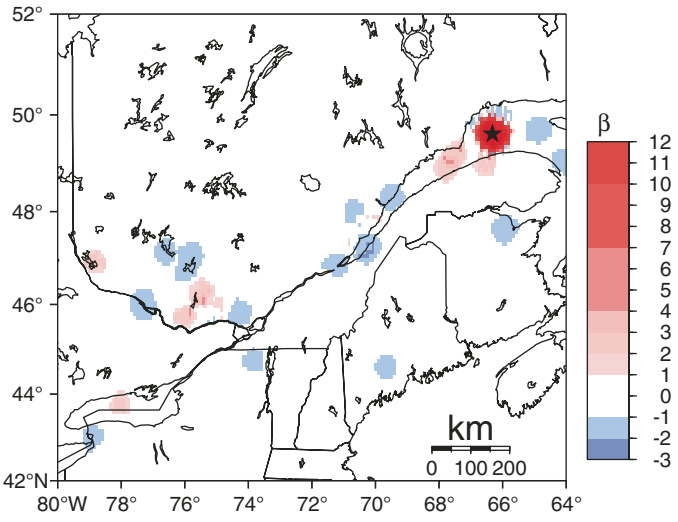

Figure 2. Beta statistic calculated from seismicity during the 30 d following the 16 March 1999 M5.1 earthquake in Quebec compared to 30 d prior to the earthquake. Scale bar indicates shading of beta values between –3 and 12. Within immediate aftershock zones, beta values are much higher. (The same scale is used for all subsequent beta-statistic maps.)

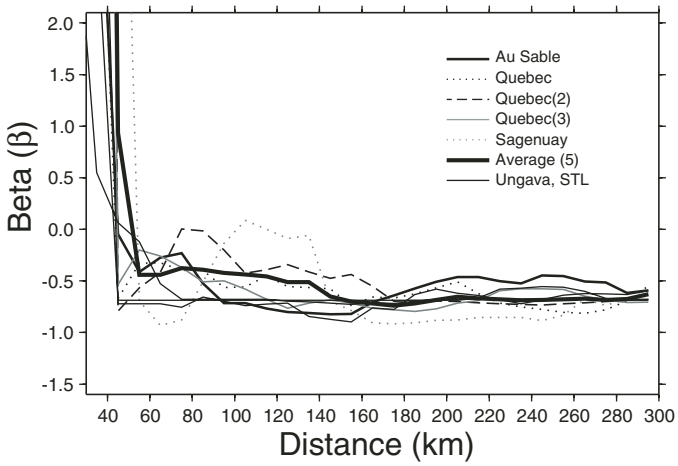

Figure 3. Beta statistic as a function of epicentral distance for the earthquakes listed in Table 1. Five of the curves reveal some hint of a molehill signal. For three events, no post–main shock seismicity was recorded outside the immediate aftershock zone: the two Ungava events and the 16 November 1997 St. Lawrence event (thin dark lines).

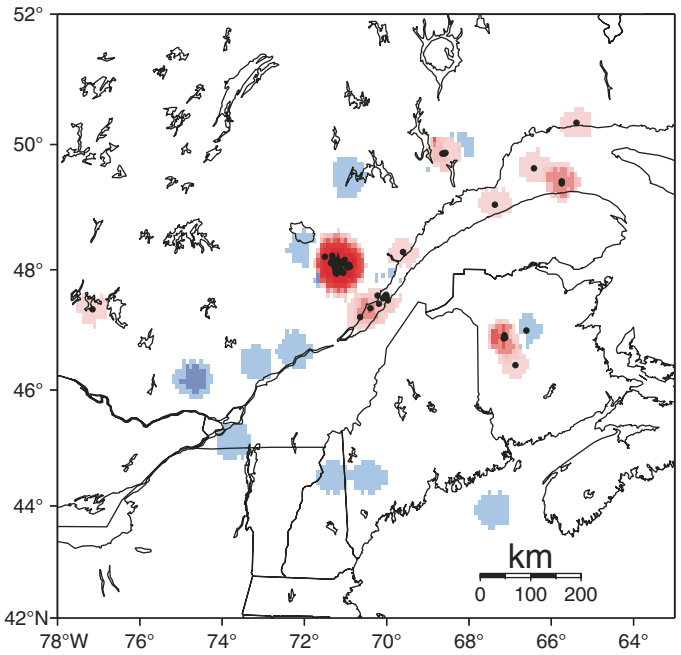

Figure 4. Seismicity following the 1988 Saguenay, Quebec, earthquake. Same color scale as shown in Figure 2.

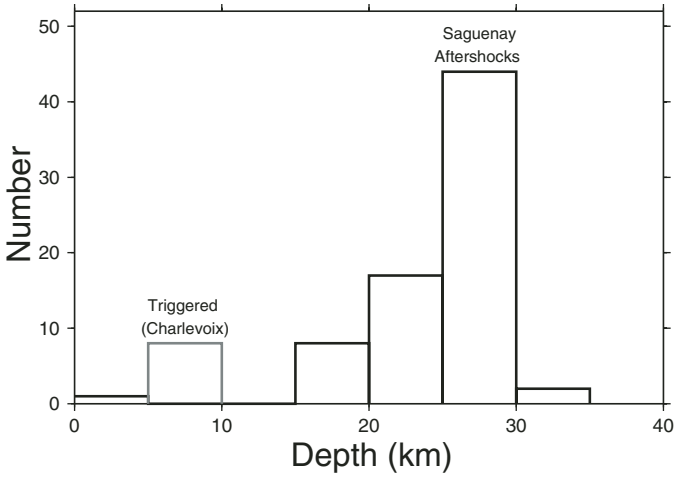

Figure 5. Histogram of depths of Saguenay aftershocks and events along the St. Lawrence shown in Figure 4 (Duberger et al., 1991). Depths (and locations) are from the Canadian National Seismic Network catalog (www.seismo.nrcan.gc.ca/cnsn), which does not report location uncertainties.

debate over the years. Early intensity surveys revealed two separate loci of strong shaking and damage suggestive of two source zones spanning a distance of 400–500 km (e.g., Middlemiss, 1905), and early magnitude estimates suggested an earthquake large enough to connect the two high-intensity regions. However, Molnar (1987) concluded that two distinct loci of high-intensity shaking were resolved by surveys following the earthquake. Moreover, Ambraseys and Bilham (2000) estimated Ms7.8 for the main shock, suggesting that the main shock rupture was not large enough to span the two high-intensity zones. As discussed by Hough et al. (2004), the extensive intensity reevaluation of Ambraseys and Douglas (2004) provided compelling additional evidence for two distinct zones of high intensity. Combined with the geodetic constraints (Bilham, 2001; Wallace et al., 2002), the macroseismic data provided compelling evidence that a substantial second event occurred near the town of Dehra Dun, ~150 km southeast of the inferred terminus of the main shock rupture. The damage near Dehra Dun was not especially severe (Ambraseys and Douglas, 2004), but by modeling predicted shaking from the main shock, Hough et al. (2004) showed that intensities were substantially higher than predicted over a broad region, including many hard rock sites. The intensity pattern was shown to be consistent with a large (M >7) earthquake at a relatively deep (30 km) depth.

As discussed by Hough et al. (2004), a small handful of early instrumental recordings are available for the Kangra earthquake. Of the handful of operating stations included in the U.S. Geological Survey (USGS) microfilm archive, seismograms are either missing for the date of the main shock or else are of poor quality, either because the reproduction quality was poor or because the data were recorded on undamped instruments that do not reveal clear phase arrivals. However, two records from early Wiechert instruments provide useful information: a recording from Gottingen included in the compilation of Duda (1992) and a recording from Leipzig, Germany (Fig. 6). The latter record is especially clear, and it reveals a sharp initial S-sS arrival followed by presumed S multiples of lower frequency. Approximately 7 min after the first S-sS arrival, a second distinct arrival can be seen on the record, very similar in frequency content and waveform characteristics to the initial S-sS group. This later arrival is clearly distinct from the main shock Love waves and is most obviously interpreted as an S-wave group from a second source. The S-sS separation is moreover larger than that in the initial S-sS group, suggesting that the second source was deeper than the first.

The available instrumental data thus corroborate the conclusions from the macroseismic data analysis and provide compelling evidence that a second substantial earthquake occurred ~7 min after the Kangra main shock, at a distance of ~150 km. Hough et al. (2004) noted that the location of the triggered earthquake coincided with a “halo” of amplified intensity that appears to have been the macroseismic signature of SmS arrivals. While this one correspondence cannot be considered a compelling piece of evidence by itself, the inferred location of the triggered earthquake is consistent with the SmS triggering hypothesis.

SmS TRIGGERING IN CALIFORNIA

The preceding results were derived from small numbers of events and are therefore regarded as intriguing but not conclusive. However, if SmS arrivals increase the likelihood of triggering, such triggering would be expected in any region where a well-defined Moho is present. Thus, to test the hypothesis of

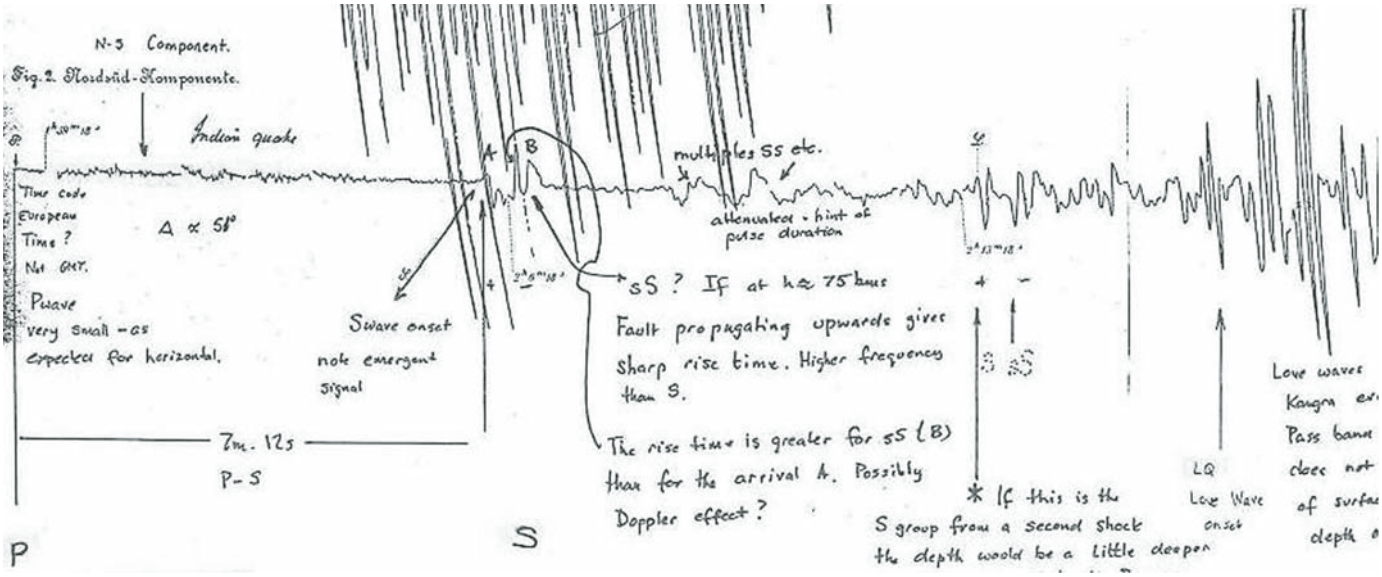

Figure 6. Seismogram of the 1905 Kangra earthquake recorded on an early Wiechert instrument in Leipzig. The record reveals a clear initial S-sS arrival, a longer-period S-multiple arrival, and a second distinct S-sS group prior to the surface waves. The S-sS separation is larger for the second group than for the first.

SmS triggering, and to explore whether remote triggering is in fact pervasive following even moderate main shocks, one can turn to a region where high seismicity rates and good catalogs are available. To investigate whether SmS triggering occurs elsewhere, I considered 27 earthquakes with magnitudes between 4.8 and 6.9 that occurred in California between 1980 and 2004, as well as the Mw7.1 Hector Mine earthquake (Table 2). I did not consider the 1992 Landers earthquake because the extent of the main shock rupture (as well as the occurrence of the Big Bear aftershock) was such that a simple distance metric could not be defined. The list of events was drawn from a compilation of significant earthquakes on the Southern California Earthquake Center (SCEC) web site (http://www.data.scec.org/chrono index/quakedex.html). Although not complete for events with magnitudes near 5, the compilation does include virtually all significant, independent moderate main shocks in southern California as well as a number of especially well-recorded M4.8–5.0 events. For events larger than M5, the SCEC list omits only aftershocks and a small number of events near the periphery of the network.

Again using the standard beta-statistic approach, I compared seismicity rates during the 30 d after and before each event. The beta statistic was calculated using a grid with 10 km spacing and a smoothing radius of 15 km. The beta-statistic maps again reveal positive and negative seismicity fluctuations outside of the aftershock zone. No widespread, statistically significant triggering is revealed for the events except for Hector Mine, consistent with previous results.

I then calculated the average beta statistic as a function of epicentral distance. Because the greater number of events allowed the possibility of more in-depth statistical analysis than was possible for the eastern Canada events, I treated the "null case" by calculating averages using only those subregions with at least one earthquake either before or after the main shock. This removed the slight negative bias introduced by the large number of cases for which seismicity rate change effectively cannot be measured, and it allows seismicity rate fluctions to be resolved against a baseline of zero.

For most of the moderate earthquakes in California, as well as the Hector Mine earthquake, β decreases outside of the immediate aftershock zone but increases slightly at a distance of 70–120 km (Fig. 7). The increase is particularly strong for the 1993 Coalinga earthquake (Fig. 8). Figure 7 also reveals a number of large peaks in β at larger distances. Although individual peaks can be large enough to affect the average, none of these peaks is as persistent as that at 70–120 km. The results shown in Figure 7 can be illustrated in map view by shifting all 27 beta-statistic maps to zero latitude/longitude and contouring the aggregate results. (Hector Mine is omitted so that the results are not biased by its relatively large aftershock zone.) Figure 9 clearly reveals that seismicity rates increase on average to a distance of at least 120 km, well beyond the traditional aftershock zone for moderate earthquakes. Seismicity also increases on average, albeit more weakly, to a distance of ~230 km.

In theory, an increase in β can result from a particularly low local standard error of the background rate. However, following earlier studies (e.g., Matthews and Reasenberg, 1988), I assumed seismicity to be Poissonian. The standard error is thus given simply as the square-root of the mean, so the increases in β described in this paper are all associated with seismicity rate increases. In effect, this approach is equivalent to a consideration of absolute seismicity rate fluctuations with an explicit normalization to background rate. In a comparison of Figures 3 and 7, it

TABLE 2. RECENT MODERATE EARTHQUAKES IN SOUTHERN AND CENTRAL CALIFORNIA ANALYZED IN THIS STUDY

Event no.	Date	Event	Mw	Lat. (°N)	Long. (°W)
1	25 February 1980	White Wash	5.5	33.50	116.52
2	26 April 1981	Westmoreland	5.8	33.096	115.625
3	15 June 1982	Anza	4.8	33.548	116.677
4	2 May 1983	Coalinga	6.1	36.228	120.318
5	8 July 1986	North Palm Springs	6.0	33.999	116.608
6	13 July 1986	Oceanside	5.5	32.971	117.874
7	1 October 1987	Whittier	5.9	34.061	118.079
9	24 November 1987	Elmore Ranch	6.2	33.090	115.792
10	26 June 1988	Upland	4.7	34.133	117.708
11	3 December 1988	Pasadena	5.0	34.141	118.133
12	19 January 1989	Malibu	5.0	33.917	118.627
13	28 June 1991	Sierra Madre	5.8	34.270	117.993
14	23 April 1992	Joshua Tree	6.1	33.960	116.317
15	11 July 1992	Mojave	5.7	35.208	118.067
16	28 May 1993	Wheeler Ridge	5.2	35.149	119.104
17	17 January 1994	Northridge	6.7	34.213	118.537
18	17 August 1995	Ridgecrest	5.4	35.776	117.662
19	27 November 1996	Coso	5.3	36.075	117.650
20	18 March 1997	Calico	5.3	34.971	116.819
21	6 March 1998	Coso	5.2	36.067	117.638
22	16 August 1998	San Bernardino	4.8	34.121	116.928
23	27 October 1998	Whiskey Springs	4.8	34.323	116.844
24	16 October 1999	Hector Mine	7.1	34.600	116.270
25	31 October 2001	Anza	5.1	33.508	116.514
26	22 February 2003	Big Bear	5.4	34.319	116.848
27	28 September 2004	Parkfield	6.0	35.819	120.364

Note: Locations and magnitudes are from SCSN/NCSN/CISN online catalogs. SCSN—Southern California Seismic Network, NCSN—Northern California Seismic Network, CISN—California Integrated Seismic Network.

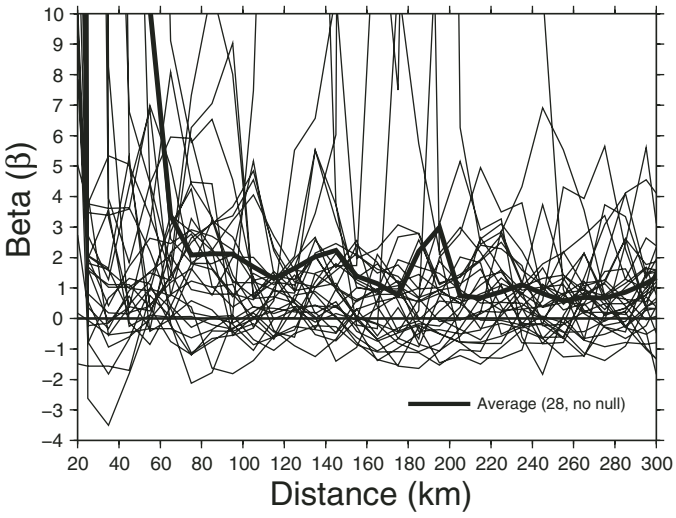

Figure 7. Beta statistic as a function of epicentral distance for 28 M4.8–7.1 earthquakes in California. Average of 28 curves is also shown (dark line).

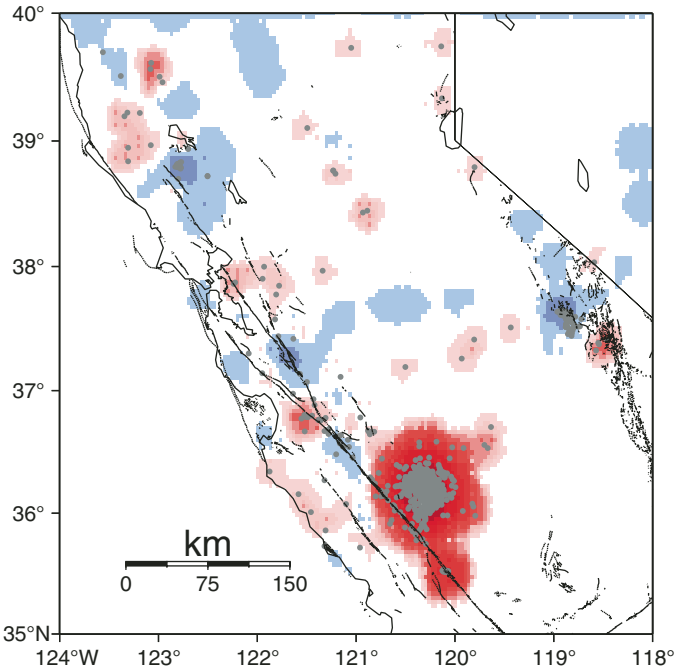

Figure 8. Beta statistic calculated from seismicity during the 30 d following the 1993 Coalinga earthquake compared to 30 d prior to the earthquake. Same color scale as shown in Figure 2.

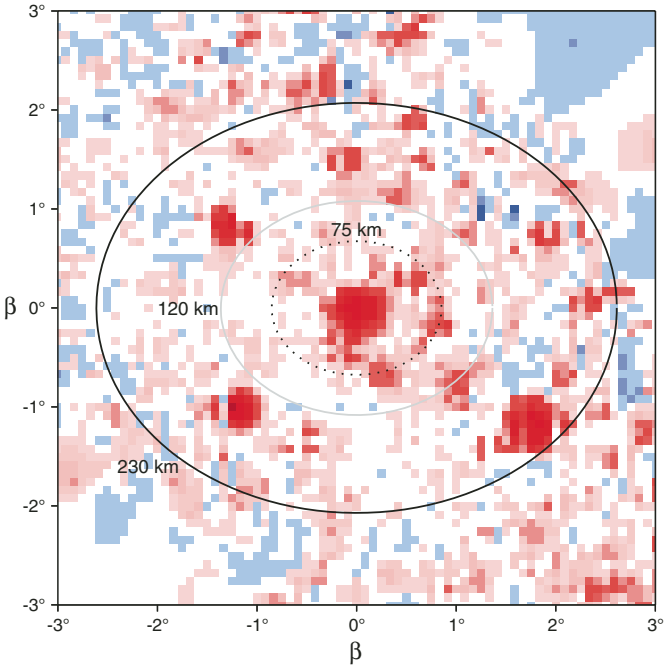

Figure 9. Average seismicity fluctuations, expressed as beta statistic, are shown in map view. To generate this (Mercator projection) map, 27 beta-statistic maps such as that shown in Figure 8 were shifted to zero origin and combined to reveal the average spatial pattern of seismicity fluctuations. The ovals correspond to three radii: (1) 75 km, the distance at which the $\beta(r)$ signal is inferred to peak slightly, (2) 120 km, the distance over which seismicity clearly increases on average, and (3) 230 km, the distance range over which average seismicity rates increase weakly.

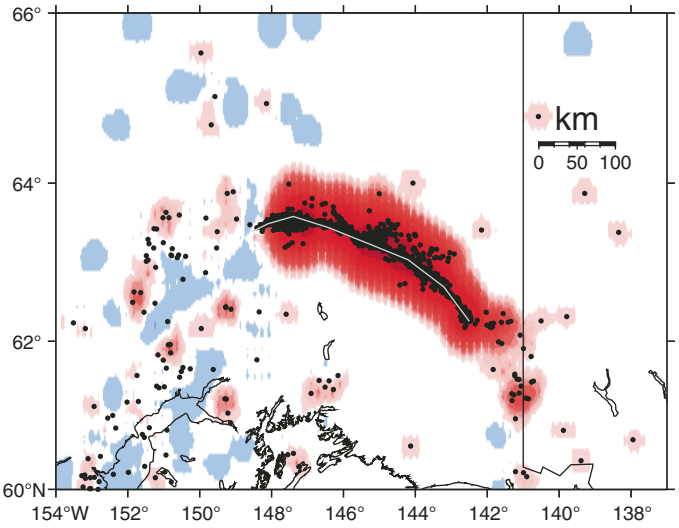

Figure 10. Seismicity fluctuations following the 2002 M7.9 Denali, Alaska, earthquake.

is clear that the molehill signature, while weak, occurs at a similar range of distances in both California and eastern North America.

Following the 2002 Denali earthquake, seismicity also increased in a region ~100–140 km to the southeast of the main shock rupture (Fig. 10). This location would have also experienced amplified ground motions due to directivity effects, which illustrates an important point: if SmS arrivals do trigger earthquakes, they will be only one of several factors that control the location of triggered events. Previous studies have shown or suggested that triggering also depends on other factors, including directivity (e.g., Kilb et al., 2000) as well as the presence of faults that are susceptible to failure.

In each of the three regions considered, the observed increases of β at 70–140 km were small, and one could not attach statistical significance to the results from any one earthquake. However, the increases were insensitive to the choice of analysis parameters (smoothing distance, etc.), and the persistent appearance of a molehill at a narrow distance range is difficult to dismiss as a fluke.

The molehill signals reflect seismicity increases within a month of the respective main shocks. The temporal sequence characteristics of remotely triggered earthquakes might provide an observational constraint against which one can test theoretical triggering models (e.g., Gomberg, 2001). However, the simplest explanation for delayed triggering is that transient stress changes cause very early triggered events, either large or small, and these initial triggered events caused local disturbances that generated local sequences (Richter, 1955; Hough and Kanamori, 2002; Hough et al., 2003). In any case, we can explore the timing of the inferred triggered earthquakes identified in this study. Following the 1983 Coalinga earthquake, the molehill was primarily due to a cluster of events to the south-southeast of the main shock (Fig. 8). The earliest recorded event in this cluster occurred ~2.5 d following the main shock. The first recorded event in the lower St. Lawrence followed the 1988 Saguenay, Quebec, main shock by a similar delay (3 d). In the absence of local broadband data, it is impossible to know if triggered earthquakes occurred in these locations immediately after their respective main shocks. However, delays ranging from a few minutes (Kangra) to a few days are consistent with the time delay of remotely triggered earthquakes observed in other regions. The triggered events identified by Hough (2001) occurred ~4 d after the 23 January 1812 main shock and ~16 and 18 h after the 7 February 1812 New Madrid main shock.

To further explore the temporal behavior of the inferred triggered earthquakes, I considered the two earthquakes that had the largest molehills: the 1983 Coalinga and 1999 Hector Mine earthquakes. Considering only the rates of earthquakes at a distance of 70 to 110 km from each main shock, I found that the rates of these events did decrease with time following their respective main shocks (Fig. 11). The time decay of the (inferred) triggered events did not change substantially when considering events between 80 and 110 km. In effect, Figure 11 suggests that the events at this distance range "look like aftershocks" in terms of their sequence statistics. However, as I discuss later, an association with SmS arrivals provides compelling evidence that these events were triggered by dynamic rather than static stress changes. In the following section, I consider the statistical significance of the observations.

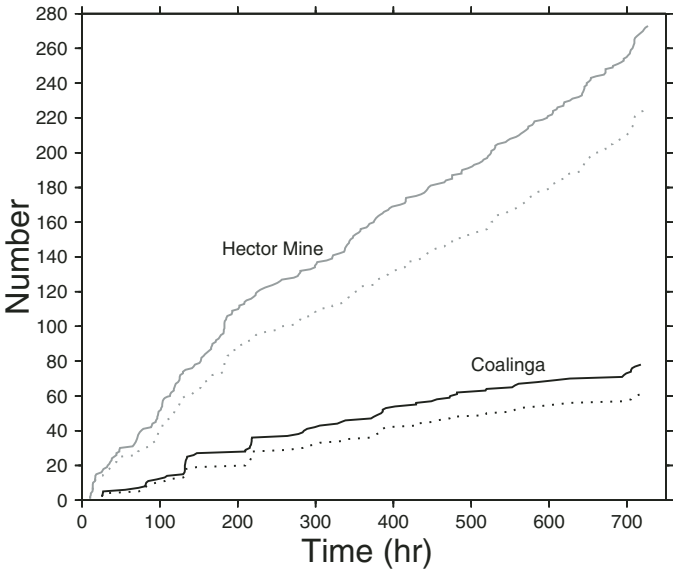

Figure 11. Cumulative number of (inferred) triggered earthquakes as a function of time following the Coalinga earthquake (black lines) and Hector Mine earthquake (gray lines). The solid lines indicate temporal characteristics of earthquakes at 70–110 km distance from the respective epicenters; the dotted lines indicate earthquakes at 80–110 km distance.

STATISTICAL SIGNIFICANCE

As previous studies have pointed out (e.g., Reasenberg and Simpson, 1992), it is difficult to assess the statistical significance of any beta-statistic result. Although one can infer strict confidence levels for different β values, β can increase or decrease substantially because of random seismicity fluctuations.

Typically, the statistical significance of seismicity observations such as those presented in this study can be demonstrated using a Monte Carlo approach whereby the results are compared to results generated with randomized catalogs. A formal Monte Carlo approach is difficult in this case, since it would clearly not be a fair test to compare the results with results from a randomized catalog. If systematic artifacts arise in $\beta(r)$, they will almost certainly be generated by the naturally clustered character of seismicity.

To explore the statistical significance of the results, I conducted the following experiment: First, I calculated beta-statistic maps for several two-month periods that included no conspicuous main shocks or swarms. I then calculated $\beta(r)$ for a series of randomly chosen test epicenters to see how often molehill signals arose. The calculations were done for suites of eight random epicenters. This number is arbitrary, and it was chosen to reflect the numbers of earthquakes analyzed in this study.

Figure 12A presents a beta-statistic map for a two-month period when seismicity did not fluctuate significantly from one month to the next. After calculating $\beta(r)$ curves for a small number of random epicenters, it became clear that there was no significant signal in $\beta(r)$. By the time the curves from the eight events were averaged, the resulting curve was nearly flat (Fig. 13).

Figure 12B presents a beta-statistic map for a two-month period in which seismicity increased modestly in some areas during the second month. Such a signal can result from either a swarm or a modest burst of events after a particularly quiet month. In this case, $\beta(r)$ can reveal peaks with amplitudes similar to those shown in Figures 3 and 7. The question is then, how likely are these signals to survive averaging over a number of randomly chosen epicenters? Again, I used eight random epicenters in each trial. Figure 14 shows the results for eight different sets of random epicenters using the map shown in Figure 12B; in each panel, the individual and average $\beta(r)$ curves are shown.

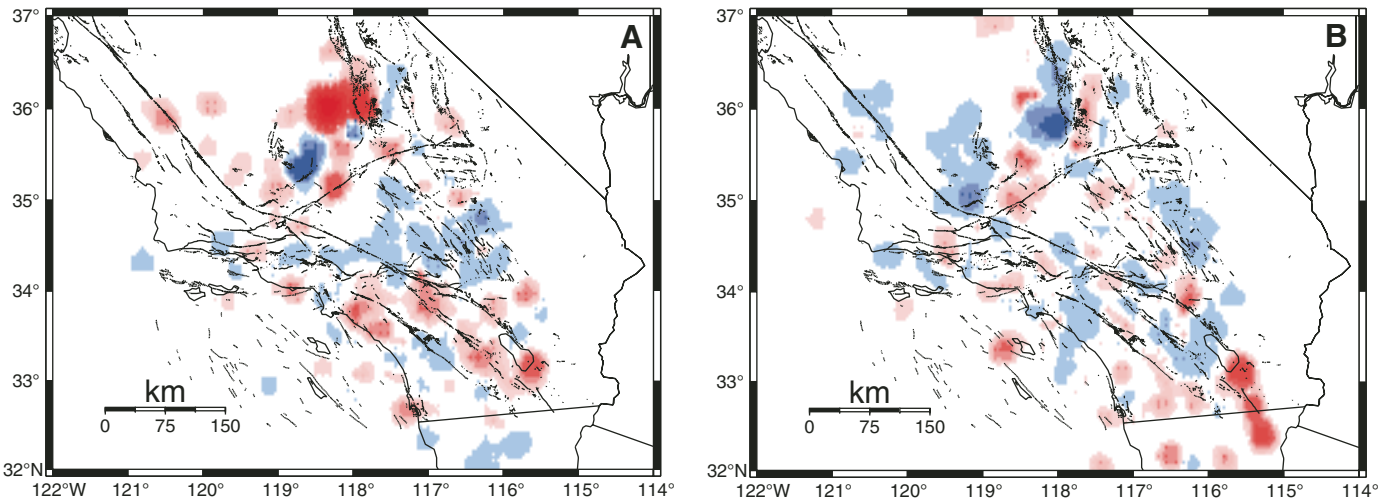

Figure 12. Beta statistic map generated using two different one-month periods during which no notable activity occurred in Southern California: March–April 2001 (A), and May–June 2001 (B). Same color scale as shown in Figure 2.

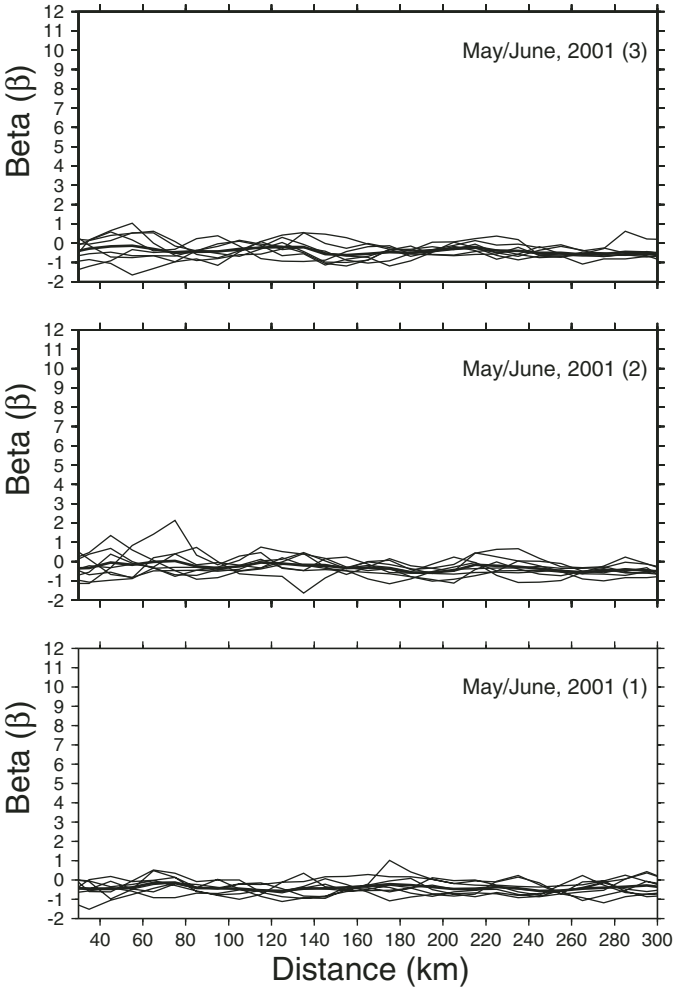

Figure 13. Using the beta-statistic map shown in Figure 12A, $\beta(r)$ curves were generated for three sets of random epicenters between 33.0°N and 35.5°N and 116°W and 119°W. Solid line in each panel indicates average of eight individual $\beta(r)$ curves.

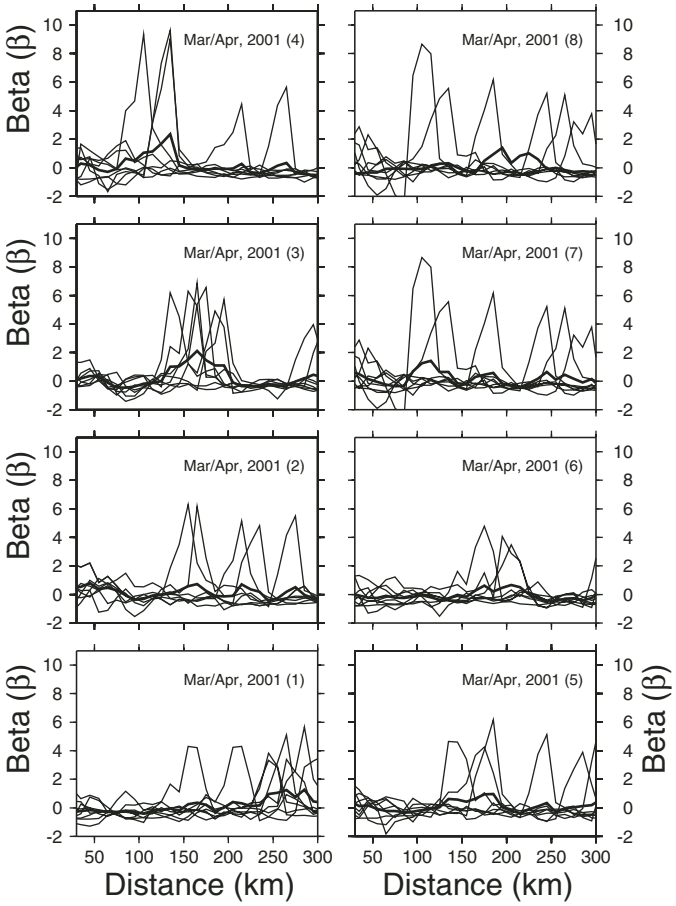

Figure 14. Using the beta-statistic map shown in Figure 12B, $\beta(r)$ curves were generated for eight sets of random epicenters between 33.0°N and 35.5°N and 116°W and 119°W. Solid line in each panel indicates average of eight individual $\beta(r)$ curves. Number in each panel, 1–8, refers to test number.

Figure 14 reveals that some systematic trends in $\beta(r)$ can arise by random chance because of random seismicity fluctuations. In test three, for example, the random epicenters happen to cluster near the center of the region, at a similar distance to the most prominent seismicity increase. However, while a hint of a persistent peak can be seen in some of the averaged curves, it occurs at a range of distances for the different simulations. The individual $\beta(r)$ curves also reveal substantial variability within any one simulation, with equally strong peaks occurring at quite different distances. These suites of curves are qualitatively different from those shown in Figures 3 and 7. The $\beta(r)$ curves in Figure 7 tend to reveal a molehill in the same distance range, or no molehill signal at all. The statistical test assumes that it is a reasonable proxy to use one beta-statistic map with multiple test epicenters instead of the same test epicenter with multiple maps. While this might be open to question, conceptually it seems clear that, if molehill signals following main shocks were simply an artifact caused by random seismicity fluctuations, those fluctuations would occur at random distances from the main shock, and the statistics would be comparable to those of the test. In fact, while this was not rigorously tested, Figures 3 and 7 provide evidence that strong, random seismicity fluctuations do not occur commonly. That is, whether or not SmS triggering occurs, if fluctuations as strong as those in Figure 13B were common, one would see $\beta(r)$ peaks at a range of distances for any given two-month period, whether or not it was centered at the time of a significant main shock. I thus conclude that, while $\beta(r)$ peaks comparable to the inferred molehills can result as artifacts due to the naturally clustered nature of seismicity, such artifacts are highly unlikely to persist in a certain, narrow distance range.

To test the significance of the inferred seismicity increase at distances over 200 km, I employed a bootstrap approach, calculating average $\beta(r)$ for random subsets of 10 events; i.e., subsets of 10 curves shown in Figure 7. The results confirm the observation that $\beta(r)$ is positive on average out to at least 200 km. Plotting the results on logarithmic axes diminishes the appearance of

the molehill signal at 70–120 km but reveals another intriguing result: the suggestion of a slope break at ~50 km (Fig. 15A). At 0–20 km, the shape of the curve will reflect finite-fault effects, as a simple epicentral distance is used. However, the slope from 20 to 50 km is systematically steeper than that at greater distances. These results appear to suggest a transition from an aftershock regime (0–50 km) to a regime in which seismicity increases are caused by triggered earthquakes. Since static stress decays as $1/r^3$, whereas the decay of dynamic stresses is closer to $1/r$, the results are consistent with the conventional interpretation that aftershocks are controlled by static stress changes, whereas remotely triggered earthquakes are controlled by dynamic stress changes. Grouping the events into 0.5-unit-magnitude bins, I found that, as expected, the distance at which the transition occurs scales with the size of the main shock (Fig. 15B).

TRIGGERED EARTHQUAKES AND SmS ARRIVALS

The fundamental result illustrated in Figure 7 is that seismicity increases to a distance of at least 200 km following moderate main shocks in California, a range that is significantly beyond a conventional aftershock zone. Thus, while seismologists have previously regarded earthquakes such as the 8 July 1986 North Palm Springs and 13 July 1986 Oceanside earthquakes as unrelated, the results presented in this study suggest otherwise. The inference of SmS triggering is therefore not surprising: if, as seems nearly certain, the probability of triggering depends on the amplitude of dynamic waves, then anything that increases wave amplitudes will increase the probability of triggering.

Several previous studies have quantified SmS amplitudes in California. Somerville and Yoshimura (1990) showed that post-critical Moho reflections, or SmS arrivals, contributed to damage in the San Francisco Bay area during the 1989 Loma Prieta, California, earthquake. Somerville and Yoshimura showed that SmS arrivals were larger than the direct S arrivals at distances of 50–100 km; later studies (e.g., Mori and Helmberger, 1996) examined recorded waveforms for the 1992 Landers earthquake and found similar results in Southern California. The distance range at which SmS waves appear depends, of course, on Moho depth. In Southern California, SmS arrivals first appear at a distance of ~70 km and can be larger than the direct S wave at distances of 70–170 km (Mori and Helmberger, 1996). Although not always larger than the direct S wave, SmS arrivals are typically of high enough amplitude to increase shaking and damage during large earthquakes (Somerville and Yoshimura, 1990; Hough et al., 2004). (At distances of 70–170 km, a distinct surface-wave group has not generally formed.)

If SmS arrivals do cause triggered earthquakes, one would expect the triggered events to occur at larger epicentral distances in regions where the Moho is deeper. The results presented in this paper are generally consistent with this hypothesis: the triggered earthquakes in eastern North America and India are at somewhat greater distances from their main shocks than the triggered earthquakes in California. However, because SmS arrivals will be of high amplitude over a range of distances, one would expect the signature of Moho depth to be smeared out.

The observations presented and summarized here provide evidence for a correspondence between the locations of remotely triggered earthquakes and the distances at which SmS waves generate large-amplitude arrivals. This correspondence has important implications. First and most fundamentally, it provides additional evidence for the earlier conclusion that triggered earth-

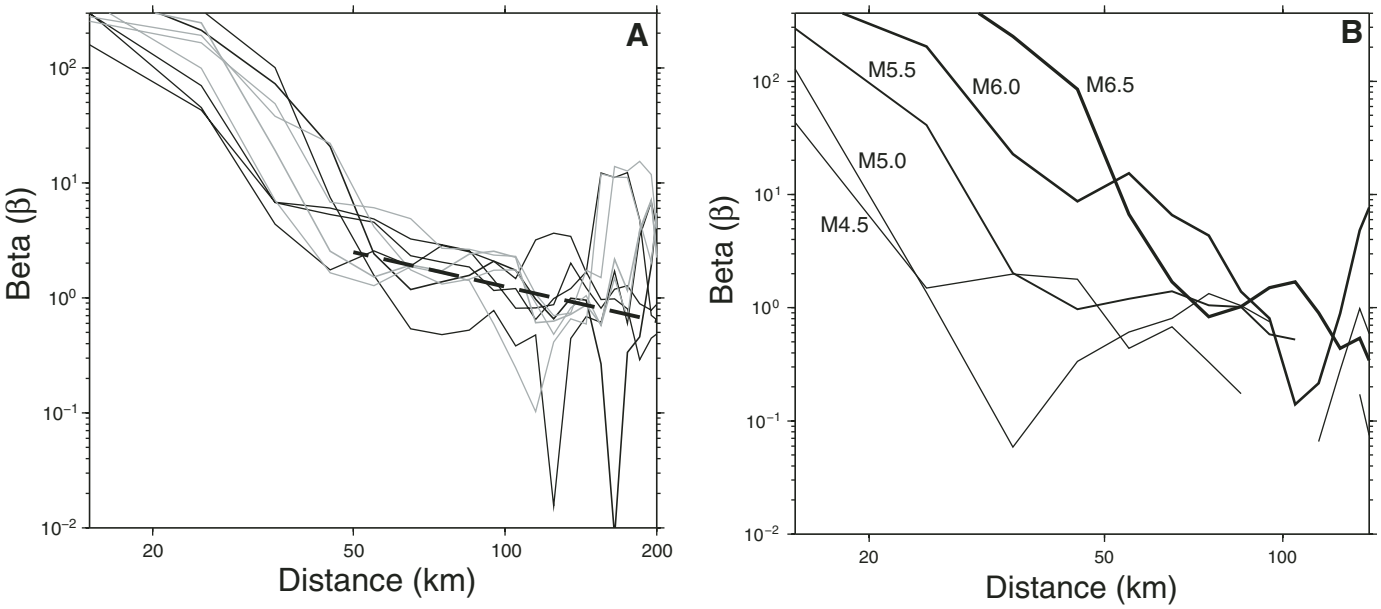

Figure 15. (A) β(*r*) curves for several suites of ten randomly chosen subsets of curves shown in Figure 7. Dark dashed line indicates a slope of −1 on logarithmic axes. (B) β(*r*) curves for California events grouped into magnitude bins, as indicated.

quakes are caused by the dynamic stress changes associated with seismic waves (e.g., Gomberg and Davis, 1996; Kilb et al., 2000; Gomberg et al., 2001), even at relatively short distances, where static stress change is not necessarily negligible.

Further, SmS waves are body waves of relatively high frequency compared to surface waves. This suggests that triggering does not (or does not always) require long-period (>10–15 s) energy, as is apparently the case in Long Valley (Brodsky and Prejean, 2004). However, it is not surprising that the nature of the triggering mechanism might be different in volcanic and nonvolcanic regions.

DISCUSSION

Observational investigations of remotely triggered earthquakes have been limited to a handful of case studies of triggering following recent large earthquakes (e.g., Hill et al., 1993; Gomberg and Davis, 1996; Kilb et al., 2000; Prejean et al., 2005). Investigations of triggering outside of volcanic or geothermal regions are more limited still, as are investigations of the source properties of remotely triggered events.

Before addressing the interpretation of remotely triggered earthquakes, it is useful to consider the implications of remotely triggered earthquake results in intraplate regions. Results to-date suggest that remotely triggered earthquakes outside of geothermal or volcanic regions occur on weak faults. Hough and Kanamori (2002) presented an analysis of remotely triggered earthquakes in the Brawley seismic zone following the 1999 Mw7.1 Hector Mine earthquake. The Brawley seismic zone is generally interpreted as an extensional transform zone in which stress is transferred between the San Andreas and Imperial faults via a zone of oblique extension (e.g., Larsen and Reilinger, 1991). Local extensional forces are associated with geothermal activity: several commercial geothermal power plants are in operation near the southern end of the Salton Sea.

Using an empirical Green's function approach to isolate source properties, Hough and Kanamori (2002) concluded that the 1999 remotely triggered earthquakes had source spectra consistent with expectations for tectonic, brittle-shear-failure earthquakes, with relatively low stress drop values of 0.1–1.0 MPa. That is, although the Brawley seismic zone is an active geothermal area, the radiated spectra of triggered earthquakes in this area do not reveal any evidence of a fluid-controlled source process. These results are not definitive: one could imagine, for example, a fluid-controlled source process that changes pore pressures within a fault zone in such a way that tectonic brittle-shear-failure earthquakes are encouraged. However, high-resolution empirical Green's function analysis can reveal evidence of anomalous source spectra of even very small earthquakes (Hough et al., 2000), and no such evidence can be seen in the triggered Brawley seismic zone events. The results are thus consistent with the simple interpretation that the earthquakes occurred on weak faults. The estimated stress drop values were generally lower than the estimated peak dynamic stress caused by the S-wave–surface-wave group. If the triggered earthquakes were total stress drop events, the peak dynamic stress exceeded the failure stress.

The inference of triggering on weak faults derives an additional measure of support from a related negative result: even relatively large, relatively close earthquakes do not appear to cause triggered earthquakes on faults such as the San Andreas (Spudich et al., 1995), although triggered slip at shallow depths is fairly common elsewhere along the San Andreas (e.g., Bodin et al., 1994; Rymer, 2000). One might argue that the San Andreas fault is itself weak; however, an interesting new elastodynamic model by Lapusta and Rice (2004) proposes that that the fault is instead brittle (statically strong but dynamically weak.) I suggest that this model provides a cohesive explanation for recent observational results concerned both triggered slip and triggered earthquakes. Triggered slip occurs on such a fault within the shallow, presumably velocity-strengthened regime, as suggested by recent modeling results (Du et al., 2003). Triggered earthquakes do not generally occur on such faults because, as demonstrated by Lapusta and Rice (2004), over most of its extent, a brittle fault will be nowhere near a failure threshold. In the model of Lapusta and Rice (2004), large earthquakes originate in the "defect regions" along a fault where, by virtue of elevated pore pressure or other material properties, the fault is especially weak. I suggest that remotely triggered earthquakes will occur in these same defect regions. By virtue of its high heat flow and extensional tectonic setting, as well as its low stress-drop events, the Brawley seismic zone is an obvious candidate for a defect region abutting the southern terminus of the San Andreas fault.

So how, then, does one explain remotely triggered earthquakes in mid-plate and collisional settings? Two possibilities exist: these events also occur at the defect regions along otherwise strong faults, and/or these events occur where faults are close to failure. As I will discuss shortly, these possibilities are not necessarily mutually exclusive. The latter interpretation was explored by Seeber (2000) and Hough et al. (2004), who showed that in a low-strain-rate environment, a small amount of permanent, aseismic deformation can keep faults close to their failure level for a longer part of the earthquake cycle than faults in high-strain-rate regions.

In the model proposed by Seeber (2000), permanent deformation is assumed to be accommodated by a mechanism such as power-law creep, the key characteristic of which is that the aseismic strain rate depends on stress. Although the real physical processes are likely to be more complex than simple power-law creep, this dependence will, regardless of the details of the mechanism, slow the accumulation of stress available to drive earthquakes. The mechanism thus provides a conceptually simple explanation for the suggestion that intraplate crust is critically stressed (e.g., Townend and Zoback, 2000), which in turn provides a straightforward conceptual explanation for remotely triggered earthquakes.

However, the possibility remains that remotely triggered earthquakes occur where faults are relatively weak. In the most compelling case of triggering in eastern Canada, the events are clustered along the St. Lawrence Seaway, a reactivated failed

Iapetan rift structure that is likely to represent a zone of relative weakness (Roy et al., 1993) in a region where faults are expected to be otherwise strong. Other (inferred) intraplate triggered earthquakes discussed in this paper are located within major river valleys; again, probable zones of (relative) weakness.

Recent results from Gangopadhyay et al. (2004) suggest that in intraplate crust, stress concentrations will develop at pre-existing zones of weakness. Using two-dimensional modeling of discrete crustal blocks, they showed how localized stress concentrations can build around zones with pre-existing intersecting faults, such as the New Madrid seismic zone. If this model is correct, remotely triggered intraplate earthquakes, like their interplate counterparts, would be expected to occur in zones of relative weakness. Unlike the situation in interplate regions, such intraplate zones would also be characterized by long-lived stress concentrations and, therefore, persistent seismicity. Remotely triggered earthquakes may thus serve as beacons of stress concentration in intraplate regions, places where future large earthquakes are possible.

In any region, remotely triggered earthquakes can provide clues into earthquake rupture processes. For example, detailed analysis of source properties could reveal whether or not intraplate triggered earthquakes, like the interplate triggered earthquakes analyzed by Hough and Kanamori (2002), are low-stress-drop events, and whether they are characterized by the more common brittle shear-failure mechanism. Further investigations of remotely triggered earthquakes in intraplate regions will also shed further light on the question of where such events do (and do not) occur.

The results presented in this paper suggest that it is not necessary to wait for rare large intraplate earthquakes to further investigate the properties of intraplate triggered earthquakes. If remotely triggered earthquakes occur more commonly than can be identified with a standard beta-statistic analysis, SmS triggering in particular provides a unique opportunity to stack signals from multiple events—perhaps as small as M5.5—and further explore the prevalence and source properties of remotely triggered earthquakes.

ACKNOWLEDGMENTS

I thank Stephanie Prejean, Jeanne Hardebeck, Karen Felzer, Ned Field, Allan Lindh, and Ross Stein for constructive feedback on the work presented in this paper.

REFERENCES CITED

Ambraseys, N., and Bilham, R., 2000, A note on the Kangra Ms = 7.8 earthquake of 4 April 1905: Current Science, v. 79, p. 101–106.

Ambraseys, N.N., and Douglas, J., 2004, Magnitude calibration of north Indian earthquakes: Geophysical Journal of the Interior, v. 159, p. 165–206, doi: 10.1111/j.1365-246X.2004.02323.x.

Bilham, R., 2001, Slow tilt reversal of the Lesser Himalaya between 1862 and 1992 at 78°E, and bounds to the southeast rupture of the 1905 Kangra earthquake: Geophysical Journal of the Interior, v. 144, p. 1–23, doi: 10.1046/j.0956-540X.2000.01255.x.

Bodin, P., and Gomberg, J., 1994, Triggered seismicity and deformation between the Landers, California, and Little-Skull-Mountain, Nevada, earthquakes: Bulletin of the Seismological Society of America, v. 84, p. 835–843.

Bodin, P., Bilham, R., Behr, J., Gomberg, J., and Hudnut, K.W., 1994, Slip triggered on Southern California faults by the 1992 Joshua Tree, Landers, and Big Bear earthquakes: Bulletin of the Seismological Society of America, v. 84, p. 806–816.

Brodsky, E.E., and Prejean, S.G., 2005, New constraints on mechanisms of remotely triggered seismicity at Long Valley Caldera: Journal of Geophysical Research, v. 110(B4), Article B04302, April.

Brodsky, E.E., Sturtevant, B., and Kanamori, H., 1998, Earthquakes, volcanos, and rectified diffusion: Journal of Geophysical Research, v. 103, p. 23,827–23,838, doi: 10.1029/98JB02130.

Das, S., and Scholz, C.H., 1981, Off-fault aftershock clusters caused by shear-stress increase: Bulletin of the Seismological Society of America, v. 71, p. 1669–1675.

Du, W.X., Sykes, L.R., Shaw, B.E., and Scholz, C.H., 2003, Triggered aseismic slip from nearby earthquakes, static or dynamic effect?: Journal of Geophysical Research, v. 108(B2): Article 2131, February.

Duberger, R., Roy, D.W., Lamontagne, M., Woussen, G., North, R.G., and Wetmiller, R.J., 1991, The Saguenay (Quebec) earthquake of November 25, 1988—Seismological data and geologic setting: Tectonophysics, v. 186, p. 59–74, doi: 10.1016/0040-1951(91)90385-6.

Duda, S.J., 1992, Global earthquakes 1903–1985: U.S. Geological Survey Open-File Report 92-360, 623 p.

Felzer, K.R., Abercrombie, R.E., and Brodsky, E.E., 2005, Testing the stress shadow hypothesis: Journal of Geophysical Research, v. 110, no. B05, S09.

Gangopadhyay, A., Dickerson, J., and Talwani, P., 2004, A two-dimensional numerical model for current seismicity in the New Madrid seismic zone: Seismological Research Letters, v. 75, p. 406–418.

Glowacka, E., Nava, F.A., de Cossio, G.D., Wong, V., and Farfan, F., 2002, Fault slip, seismicity, and deformation in Mexicali Valley, Baja California, Mexico, after the M7.1 1999 Hector Mine earthquake: Bulletin of the Seismological Society of America, v. 92, p. 1290–1299.

Gomberg, J., 2001, The failure of earthquake failure models: Journal of Geophysical Research, v. 106, p. 16,253–16,263, doi: 10.1029/2000JB000003.

Gomberg, J., and Davis, S., 1996, Strain changes and triggered seismicity following the M(w)7.3 Landers, California, earthquake: Journal of Geophysical Research, v. 101, p. 751–764, doi: 10.1029/95JB03251.

Gomberg, J., Reasenberg, P.A., Bodin, P., and Harris, R.A., 2001, Earthquake triggering by seismic waves following the Landers and Hector Mine earthquakes: Nature, v. 411, p. 462–466, doi: 10.1038/35078053.

Gomberg, J., Bodin, P., Larson, K., and Dragert, H., 2004, Earthquake nucleation by transient deformations caused by the M = 7.9 Denali, Alaska, earthquake: Nature, v. 427, p. 621–624, doi: 10.1038/nature02335.

Hill, D.P., Reasenberg, P.A., Michael, A., Arabaz, W.J., Beroza, G., Brunmbaugh, D., Brune, J.N., Castro, R., Davis, S., DePolo, D., Ellsworth, W.L., Gomberg, J., Harmsen, S., House, L., Jackson, S.M., Johnston, M.J.S., Jones, L., Keller, R., Malone, S., Munguia, L., Nava, S., Pechmann, J.-C., Sanford, A., Simpson, R.W., Smith, R.B., Stark, M., Stickney, M., Vidal, A., Walter, S., Wong, V., and Zollweg, J., 1993, Seismicity remotely triggered by the magnitude 7.3 Landers, California, earthquake: Science, v. 260, p. 1617–1623, doi: 10.1126/science.260.5114.1617.

Hough, S.E., 2001, Triggered earthquakes and the 1811–1812 New Madrid, central U.S. earthquake sequence: Bulletin of the Seismological Society of America, v. 91, p. 1574–1581, doi: 10.1785/0120000259.

Hough, S.E., and Kanamori, H., 2002, Source properties of earthquakes near the Salton Sea triggered by the 16 October 1999 M7.1 Hector Mine earthquake: Bulletin of the Seismological Society of America, v. 92, p. 1281–1289, doi: 10.1785/0120000910.

Hough, S.E., Dollar, R., and Johnson, P., 2000, The 1998 earthquake sequence south of Long Valley Caldera, California: Hints of magmatic involvement: Bulletin of the Seismological Society of America, v. 90, p. 752–763, doi: 10.1785/0119990109.

Hough, S.E., Seeber, L., and Armbruster, J.G., 2003, Intraplate triggered earthquakes: Observations and interpretation: Bulletin of the Seismological Society of America, v. 93, p. 2212–2221.

Johnston, A.C., 1996, Seismic moment assessment of earthquakes in stable continental regions. III: New Madrid 1811–1812, Charleston 1886, and Lisbon 1755: Geophysical Journal of the Interior, v. 126, p. 314–344.

Johnston, A.C., and Schweig, E.S., 1996, The enigma of the New Madrid earthquakes of 1811–1812: Annual Reviews of Earth and Planetary Science Letters, v. 24, p. 339–384, doi: 10.1146/annurev.earth.24.1.339.

Kilb, D., Gomberg, J., and Bodin, P., 2000, Triggering of earthquake aftershocks by dynamic stresses: Nature, v. 408, p. 570–574, doi: 10.1038/35046046.

King, G.C.P., Stein, R.S., and Lin, J., 1994, Static stress changes and the triggering of earthquakes: Bulletin of the Seismological Society of America, v. 84(3), p. 935–953.

Larsen, S., and Reilinger, R., 1991, Age constraints for the present fault configuration of the Imperial Valley, California—Evidence for northwestward propagation of the Gulf of California rift system: Journal of Geophysical Research, v. 96, p. 10,339–10,346.

Linde, A.T., Sacks, I.S., Johnston, M.J.S., Hill, D.P., and Bilham, R.G., 1994, Increased pressure from rising bubbles as a mechanism for remotely triggered seismicity: Nature, v. 371, p. 408–410, doi: 10.1038/371408a0.

Lapusta, N., and Rice, J.R., 2003, Nucleation and early seismic propagation of small and large events in a crustal earthquake model: Journal of Geophysical Research, v. 108(B4), 2205, doi: 10.1029/2001JB000793.

Matthews, M.V., and Reasenberg, P.A., 1988, Statistical methods for investigating quiescence and other temporal seismicity patterns: Pure and Applied Geophysics, v. 126, p. 357–372, doi: 10.1007/BF00879003.

Mauk, F., Christensen, D., and Henry, S., 1982, The Sharpsburg, Kentucky, earthquake 27 July 1980: Main shock parameters and isoseismal maps: Bulletin of the Seismological Society of America, v. 72, p. 221–236.

Middlemiss, C.S., 1905, Preliminary account of the Kangra earthquake of 4th April: Memoir of the Geological Society of India 32, part 4: Calcutta, Geological Survey of India, p. 258–294.

Molnar, P., 1987, The distribution of intensity associated with the 1905 Kangra earthquake and bounds on the extent of rupture: Journal of the Geological Society of India, v. 29, p. 221.

Mori, J., and Helmberger, D., 1996, Large-amplitude Moho reflections (SmS) from Landers aftershocks, Southern California: Bulletin of the Seismological Society of America, v. 86, p. 1845–1852.

Mueller, K., Hough, S.E., and Bilham, R., 2004, Analysing the 1811–1812 New Madrid earthquakes with recent instrumentally recorded aftershocks: Nature, v. 429, p. 284–288, doi: 10.1038/nature02557.

Power, J.A., Moran, S.C., McNutt, S.R., Stihler, S.D., and Sanchez, J.J., 2001, Seismic response of the Katmai volcanos to the 6 December 1999 magnitude 7.0 Karluk Lake earthquake, Alaska: Bulletin of the Seismological Society of America, v. 91, p. 57–63, doi: 10.1785/0120000054.

Prejean, S.G., Hill, D.P., Brodsky, E.E., Hough, S.E., Johnston, M.J.S., Malone, S.D., Oppenheimer, D.H., Pitt, A.M., and Richards-Dinger, K.B., 2005, Remotely triggered seismicity on the United States West Coast following the M7.9 Denali fault earthquake: Bulletin of the Seismological Society of America, v. 94, p. S348–S359, doi: 10.1785/0120040610.

Reasenberg, P.A., and Simpson, R.W., 1992, Response of regional seismicity to the static stress change produced by the Loma-Prieta earthquake: Science, v. 255, p. 1687–1690, doi: 10.1126/science.255.5052.1687.

Richter, C.F., 1955, Unpublished notes, Box 7.8, Papers of Charles F. Richter, 1839–1984: Pasadena, California Institute of Technology Archives.

Roy, D.W., Schmitt, L., Woussen, G., and Duberger, R., 1993, Lineaments from airborne SAR images and the 1988 Saguenay earthquake, Quebec, Canada: Photogrammetric Engineering and Remote Sensing, v. 59(8), p. 1299–1305.

Rymer, M.J., 2000, Triggered surface slips in the Coachella Valley area associated with the 1992 Joshua Tree and Landers, California, earthquakes: Bulletin of the Seismological Society of America, v. 90, p. 832–848, doi: 10.1785/0119980130.

Scholz, C.H., 2003, Earthquakes—Good tidings: Nature, v. 425, p. 670–671, doi: 10.1038/425670a.

Seeber, L., 2002, Triggered earthquakes and hazard in stable continental regions: Vicksburg, Mississippi, Report to U.S. Army Corps of Engineers, Waterways Experiment Station, 40 p.

Seeber, L., and Armbruster, J.G., 1987, The 1886–1889 aftershocks of the Charleston, South Carolina, earthquake—A widespread burst of seismicity: Journal of Geophysical Research, v. 92, p. 2663–2696.

Somerville, P., and Yoshimura, J., 1990, The influence of critical Moho reflections on strong ground motions recorded in San Francisco and Oakland during the 1989 Loma Prieta earthquake: Geophysical Research Letters, v. 17, p. 1203–1206.

Spudich, P., Steck, L.K., Hellweg, M., Fletcher, J.B., and Baker, L.M., 1995, Transient stresses at Parkfield, California, produced by the M-7.4 Landers earthquake of June 28, 1992—Observations from the UPSAR dense seismogram array: Journal of Geophysical Research, v. 100, p. 675–690, doi: 10.1029/94JB02477.

Stark, M.A., and Davis, S.D., 1996, Remotely triggered microearthquakes at The Geysers geothermal field, California: Geophysical Research Letters, v. 23, p. 945–948, doi: 10.1029/96GL00011.

Sturtevant, B., Kanamori, H., and Brodsky, E.E., 1996, Seismic triggering by rectified diffusion in geothermal systems: Journal of Geophysical Research, v. 101, p. 25,269–25,282, doi: 10.1029/96JB02654.

Toda, S., and Stein, R.S., 2003, Toggling of seismicity by the 1997 Kagoshima earthquake couplet: A demonstration of time-dependent stress transfer: Journal of Geophysical Research, v. 108(B12): Article 2567, Dec.

Townend, J., and Zoback, M., 2000, How faulting keeps the crust strong: Geology, v. 28, p. 399–402.

Wallace, K., Bilham, R., Blume, F., Gaur, V.K., and Gahalaut, V., 2005, Surface deformation in the region of the 1905 Kangra Mw = 7.8 earthquake in the period 1846–2001: Geophysical Research Letters, v. 32 (15), Article L15307, August.

Manuscript Accepted by the Society 29 November 2006